

The zirconium and hafnium monochlorides are further remarkable in that they are the first evidently metallic halides prepared which are not iodides (other than  $\text{Ag}_2\text{F}$ ).<sup>18</sup> The small net paramagnetism of  $\text{HfCl}$ ,  $53 \times 10^{-6}$  emu mol<sup>-1</sup>, is typical of (but not conclusive evidence for) a Pauli contribution in a metallic salt; for example, compare  $104 \times 10^{-6}$  and  $50 \times 10^{-6}$  for  $\text{LaI}_2$  and  $\text{ThI}_2$ , respectively.<sup>18,19</sup> Qualitative evidence suggests that the two monochloride phases near the oxidized limit of their homogeneity ranges are more paramagnetic.

It is significant to note that  $\text{ZrCl}$  is nominally iso-electronic with  $\text{NbO}$  which is also metallic but which possesses a simple cubic structure.<sup>20</sup> However, the greater size of the chloride atom in  $\text{ZrCl}$  would likely prevent or distort the square coordination of metal

(18) J. D. Corbett, R. A. Sallach, and D. A. Lokken, *Advances in Chemistry Series*, No. 71, American Chemical Society, Washington, D. C., 1967, p 56.

(19) R. J. Clark and J. D. Corbett, *Inorg. Chem.*, **2**, 460 (1963).

(20) H. Schäfer and H. G. Schnering, *Angew. Chem.*, **76**, 845 (1964).

about the nonmetal which is found in the  $\text{NbO}$  structure if maintenance of metal-metal distances of 2.9–3.0 Å is essential for stable bonding.

The nonexistence of a dichloride of hafnium is consistent with the absence of a diiodide as well.<sup>2</sup> On the other hand, diverse attempts to prepare a hafnium monoiodide were unsuccessful, and, judging from conditions necessary to form  $\text{HfCl}$ , the compound should probably have formed in earlier studies were it stable. The results are, of course, in contrast with the usual guideline that compounds of the heavier halides are more stable with respect to disproportionation, but this generality disregards specific electronic effects.

**Acknowledgment.**—The authors are indebted to Professor E. M. Larsen for not only calling Zirklor to our attention but also furnishing literature and a sample. Professor R. E. McCarley and E. T. Maas generously guided us in the use of their Faraday balance.

CONTRIBUTION FROM THE DEPARTMENT OF CHEMISTRY,  
UNIVERSITY OF MARYLAND, COLLEGE PARK, MARYLAND 20742

## Vibrational Spectra of Single-Crystal Sodium Nitroprusside. II. Polarized Infrared Spectra and Normal-Coordinate Analysis<sup>1a</sup>

By JOHN B. BATES<sup>1b</sup> AND R. K. KHANNA

Received December 1, 1969

The polarized infrared spectra of a single crystal of sodium nitroprusside ( $\text{Na}_2\text{Fe}(\text{CN})_5\text{NO} \cdot 2\text{H}_2\text{O}$ ) were measured from 300 to 4000  $\text{cm}^{-1}$  at 300°K. The results of these measurements along with the results of a normal-coordinate analysis provide sufficient data for a complete interpretation of the vibrational spectra of the  $\text{Fe}(\text{CN})_5\text{NO}^{2-}$  ion in the solid state. The observed splitting of the vibrational modes of HDO (included as water of hydration in crystalline sodium nitroprusside) is interpreted as due to an orientational effect.

### Introduction

In a previous report by R. K. K., *et al.*,<sup>2</sup> the results of investigations of the Raman spectra of an oriented single crystal and the infrared spectra of a polycrystalline sample of sodium nitroprusside were described. On the basis of the observed relative intensities of the Raman-active phonons in the spectra with different polarizability (derivative) components and a comparison with the infrared spectra, an attempt was made to obtain the frequencies of the normal modes of the  $\text{Fe}(\text{CN})_5\text{NO}^{2-}$  ion. Some of the assignments, particularly in the region 600–300  $\text{cm}^{-1}$ , remained tentative in ref 2 because of the lack of polarization data in the infrared spectra and because of extreme weakness of the Raman-active phonons in this region. Also, the fine structure of the  $\text{H}_2\text{O}$  bands in the infrared spectra (reported in ref 2) was tentatively interpreted as due to

correlation field splitting. An interesting feature of the infrared spectra of the partially deuterated sample of sodium nitroprusside is the fine structure observed for each of the HDO vibrational modes. This fine structure cannot be due to correlation field splitting, and its interpretation was omitted in ref 2.

We have now completed the study of the polarized infrared spectra of sodium nitroprusside in the region 4000–300  $\text{cm}^{-1}$ . The assignments proposed in ref 2 will be considered in view of these results and a normal-coordinate analysis of the  $\text{Fe}(\text{CN})_5\text{NO}^{2-}$  ion. In addition, we shall also provide an explanation for the splitting of the HDO vibrational modes observed in ref 2.

### Experimental Section

Single crystals of sodium nitroprusside were grown as described in ref 2. Because of strong infrared absorptions by the  $\text{Fe}(\text{CN})_5\text{NO}^{2-}$  ion, the crystal face perpendicular to the radiation beam required polishing to a very thin section. Thus, two crystal specimens were prepared, one having the *ab* face perpendicular to the beam and the other having the *bc* face perpen-

(1) (a) Supported by a grant from ARPA, Department of Defense. (b) Chemistry Division, Oak Ridge National Laboratory, Oak Ridge, Tenn.

(2) R. K. Khanna, C. W. Brown, and L. H. Jones, *Inorg. Chem.*, **8**, 2195 (1969).

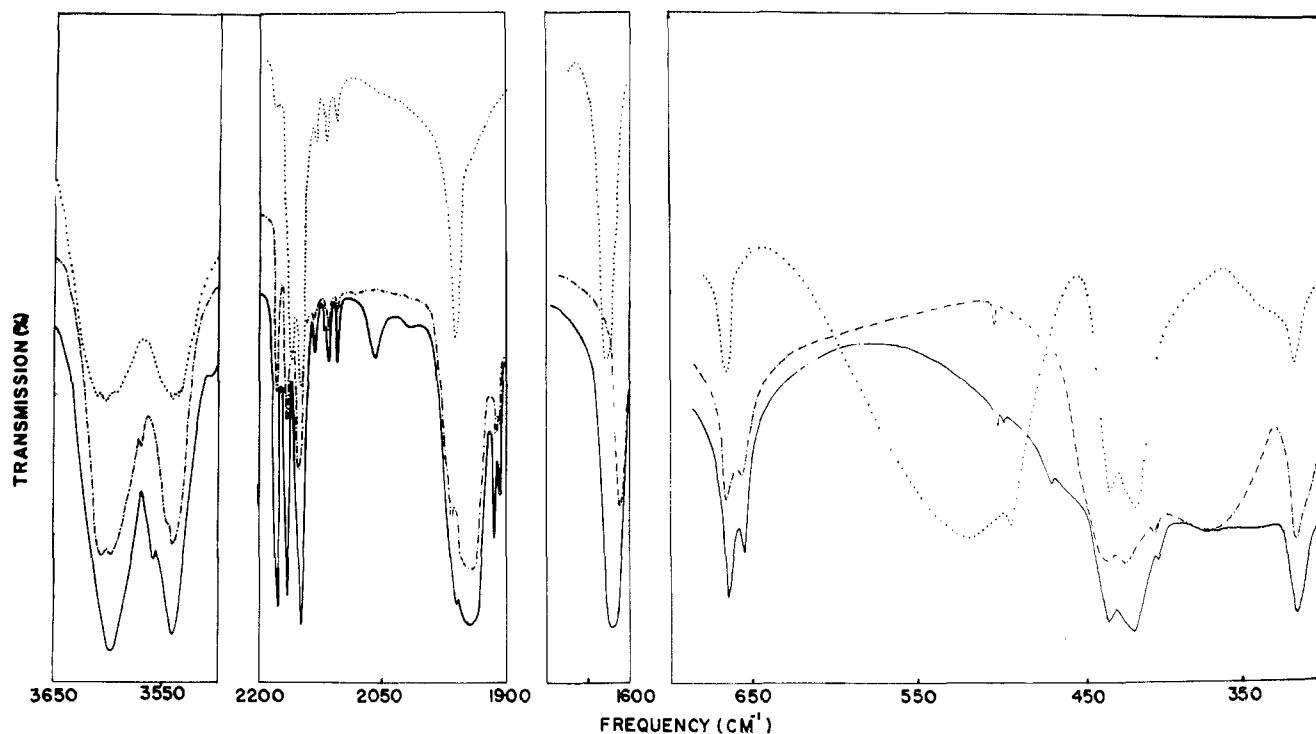


Figure 1.—Polarized infrared spectra of single-crystal sodium nitroprusside: —, polarization parallel to  $a$ ; ---, polarization parallel to  $b$ ; ···, polarization parallel to  $c$ .

pendicular to the beam. All measurements were made at 300°K on a Perkin-Elmer 225 grating spectrophotometer equipped with both an AgBr and a polyethylene polarizer. Spectra were recorded with the incident beam polarized parallel to the  $a$ ,  $b$ , and  $c$  crystal axes on successive runs. The overall resolution on each run was  $1.5 \text{ cm}^{-1}$ , and the overall accuracy was  $\pm 2 \text{ cm}^{-1}$ .

The results of the polarization measurements are collected in Table I, and traces of the spectra are presented in Figure 1. Because each of the two crystal faces used in obtaining the spectra had the  $b$  axis in common, a comparison of the relative intensities of the bands observed in the three polarized spectra could be made.

### Discussion

**A. Polarized Ir Spectra.**—From the crystal structure determination of Manoharan and Hamilton,<sup>3</sup> sodium nitroprusside crystallizes in the orthorhombic system with space group  $Pn\bar{m}$  ( $D_{2h}^{12}$ ), and the primitive cell contains four  $\text{Na}_2\text{Fe}(\text{CN})_5\text{NO}\cdot 2\text{H}_2\text{O}$  formula units. The  $\text{Fe}(\text{CN})_5\text{NO}^{2-}$  ions occupy sites of  $C_s$  symmetry, and the  $\text{H}_2\text{O}$  molecules occupy  $C_1$  sites.<sup>3</sup> The 33 vibrational modes of  $\text{Fe}(\text{CN})_5\text{NO}^{2-}$  are distributed among the symmetry species of the  $C_{4v}$  point group as

$$\Gamma = 8 A_1 + A_2 + 4 B_1 + 2 B_2 + 9 E$$

Only the  $A_1$  and  $E$  modes are infrared active under  $C_{4v}$  selection rules, but the  $A_2$ ,  $B_1$ , and  $B_2$  modes are expected to show activity in the crystal.<sup>2</sup> The correlation diagram given in Table III of ref 2 predicts the following results for the polarized ir spectra:  $A_1$  and  $B_2$  modes should each exhibit two correlation field components polarized along the  $a$  and  $b$  crystal axes. The  $A_2$  and  $B_1$  modes should each exhibit one correlation field component polarized parallel to the  $c$  crystal axis,

TABLE I  
POLARIZED INFRARED SPECTRUM OF SINGLE-CRYSTAL  
 $\text{Na}_2\text{Fe}(\text{CN})_5\text{NO}\cdot 2\text{H}_2\text{O}$  MEASURED AT 300°K<sup>a</sup>

Freq, $\text{cm}^{-1}$			Assignment
$\parallel a$	$\parallel b$	$\parallel c$	
3630 vb	3630 vb	3630 vb	$\nu_3'(\text{H}_2\text{O})$
3580 sh	3580 sh	3580 sh	
3550 vb	3550 vb	3550 vb	$\nu_1'(\text{H}_2\text{O})$
2173 s	2173 m		$\nu_1(A_1)[\text{CN}(\text{axial})]$
2162	2162		$\nu_2(A_1)[\text{CN}(\text{radial})]$
		2157	$\nu_{10}(B_1)[\text{CN}(\text{radial})]$
2143	2143	2143	$\nu_{16}(E)[\text{CN}(\text{radial})]$
1963	1963	1963	Longitudinal mode of $\nu_3$
1945 s	1945 m		$\nu_3(A_1)(\text{NO})$
		1624	$\nu_2'(\text{H}_2\text{O})$
1618			
	1614		
665	665	665	$\nu_{21}(E), \gamma, \delta(\text{FeNO})$
654 m	654 w		$\nu_6(A_1)(\text{FeN})$
515 w	515 w	515 s, vb	$\nu_2(\text{H}_2\text{O})$
501			$\nu_5(A_1), \theta(\text{FeCN})$
494		494	$\nu_{20}(E), \gamma', \delta'(\text{FeCN})$
468 m	468 w		$\nu_7(A_1)[\text{FeC}(\text{axial})]$
436	434	432	$\nu_{19}(E), \theta(\text{FeCN})$
421	421	418	$\nu_{17}(E)[\text{FeC}(\text{radial})]$
405	405		$\nu_5(A_1)[\text{FeC}(\text{radial})]$
370	370		$\nu_{14}(B_2), \lambda(\text{FeCN}), L(\text{H}_2\text{O})$
		335	$\nu_9(A_2), \lambda(\text{FeCN}), L(\text{H}_2\text{O})$
322	322	322	$\nu_{18}(E), \lambda(\text{FeCN})$

<sup>a</sup>  $\parallel a$ ,  $\parallel b$ , and  $\parallel c$  denote incident radiation parallel to the  $a$ ,  $b$ , and  $c$  crystal axes, respectively. Abbreviations: b, broad; m, medium; s, strong; sh, shoulder; vb, very broad. L denotes a lattice mode.

and each  $E$  mode should show three correlation field components polarized along the  $a$ ,  $b$ , and  $c$  crystal axes, respectively. The atoms located along the  $C_4$  axis of the free nitroprusside ion,  $\text{ONFeCN}$  (Figure 3 of ref 2),

(3) P. T. Manoharan and W. C. Hamilton, *Inorg. Chem.*, **2**, 1043 (1963).

lie in the  $ab$  crystal plane, and this axis is inclined to the  $a$  and  $b$  crystal axes at angles of about 36 and 54°, respectively.<sup>2,3</sup> Thus, in the oriented gas approximation, we can expect the intensities of the NO, FeN, and CN axial stretching modes to be greater for polarization parallel to  $a$  than for polarization parallel to  $b$ .

The group theory and intensity predictions outlined above provided the basis for assigning the polarized infrared data given in Table I. As we shall point out later, these assignments are also supported by the normal-coordinate analysis.

The polarization characteristics of the bands at  $\sim 2173$ , 2162, 2157, and 2143  $\text{cm}^{-1}$  are consistent with their assignments to  $\nu_1(A_1)$ ,  $\nu_2(A_1)$ ,  $\nu_{10}(B_1)$ , and  $\nu_{16}(E)$  CN stretches, respectively, as proposed in ref 2 and in an earlier report on the polarized infrared spectrum of sodium nitroprusside in the CN stretching region.<sup>4</sup> Similarly, the polarization characteristics of the bands at  $\sim 665$  and 654  $\text{cm}^{-1}$  are consistent with the earlier assignment of these to  $\nu_{21}(E)$  and  $\nu_6(A_1)$ , respectively.<sup>2,5</sup>

The 1945- $\text{cm}^{-1}$  band appears strongly in the  $a$  and  $b$  polarized spectra and its assignment to the  $\nu_3(A_1)$  NO stretch agrees with the isotopic shifts reported in ref 2. A shoulder at  $\sim 1963$   $\text{cm}^{-1}$  appears in all three polarized spectra and is, presumably, due to the longitudinal phonon associated with NO stretch and arising due to convergence of the incident radiation beam.<sup>6</sup> A band reported at  $\sim 1950$   $\text{cm}^{-1}$  in the spectrum of the polycrystalline sample (Table II of ref 2) was found to shift in frequency and vary in intensity depending upon how the mull was prepared. Such behavior is characteristic of strongly polar modes of ionic crystals where a combined effect of absorption, reflection, and scattering (dependent on particle size and shape) results in a shift of the absorption maxima from the true transverse phonon frequency.<sup>7</sup>

The region between 600 and 300  $\text{cm}^{-1}$  is highly complex partly due to strong absorption by the  $\text{H}_2\text{O}$  torsional modes and partly due to mixing of the modes of same symmetry species. Therefore, the assignments in this region are based on intensity considerations and normal-coordinate analysis in addition to the polarization data. The polarization data in the region 600–400  $\text{cm}^{-1}$  agree with those reported by Tos.,<sup>8</sup> small frequency differences being, presumably, due to the breadth of the bands. Although this work escaped our attention in the preparation of ref 2, an analysis of the data was not given in ref 8. The polarization data provide assignments for  $\nu_{18}(E)$  and  $\nu_{19}(E)$  (Table II) which were not obvious in ref 2. The assignments of  $\nu_9(A_2)$ ,  $\nu_{12}(B_1)$ , and  $\nu_{14}(B_2)$  are based on the low-temperature infrared spectrum which gives some weak and sharp maxima appearing as shoulders of the stronger bands. Since  $A_2$ ,  $B_1$ , and  $B_2$  species of the point group  $C_{4v}$  are infrared inactive, the weak shoulders may be due to the activity of these modes in the crystal lattice.

TABLE II  
OBSERVED AND CALCULATED FREQUENCIES FOR THE  
 $\text{Fe}(\text{CN})_5\text{NO}^{2-}$  ION IN THE CRYSTAL AT 300°

Symmetry species	Mode no. <sup>a</sup>	Freq, $\text{cm}^{-1}$			Primary contributor <sup>b</sup>	
		Polarized ir	Raman <sup>2</sup>	Calcd		
A <sub>1</sub>	$\nu_1$	2173	2174	2174	$\nu$ [CN(axial)]	
	$\nu_2$	2162	2162	2164	$\nu$ [CN(radial)]	
	$\nu_3$	1947	1947	1947	$\nu$ (NO)	
	$\nu_4$	405	408	411	$\nu$ [FeC(radial)]	
	$\nu_5$	468	472	472	$\nu$ [FeC(axial)]	
	$\nu_6$	654	656	656	$\nu$ (FeN)	
	$\nu_7$	501	493	460	$\theta$ (FeCN)	
	$\nu_8$		123	127	$\beta'$ (CFeC), $\beta$ (CFeN)	
A <sub>2</sub>	$\nu_9$	335 <sup>c</sup>	...	323	$\lambda$ (FeCN)	
B <sub>1</sub>	$\nu_{10}$	2157	2157	2164	$\nu$ [CN(radial)]	
	$\nu_{11}$	410	410	412	$\nu$ [FeC(radial)]	
	$\nu_{12}$	459	...	460	$\theta$ (FeCN)	
	$\nu_{13}$	...	125	100	$\beta$ (CFeN), $\beta'$ (CFeC)	
B <sub>2</sub>	$\nu_{14}$	370 <sup>c</sup>	...	377	$\lambda$ (FeCN)	
	$\nu_{15}$	...	100	91	$\alpha$ (CFeC)	
E	$\nu_{16}$	2143	2143	2136	$\gamma$ [CN(radial)]	
	$\nu_{17}$		420	422	$\nu$ [FeC(radial)]	
	$\nu_{18}$		322	...	335	$\lambda$ (FeCN)
	$\nu_{19}$		436	...	441	$\theta$ (FeCN)
	$\nu_{20}$		494	(415) <sup>d</sup>	496	$\gamma'$ , $\delta'$ (FeCN)
	$\nu_{21}$		665	665	667	$\gamma$ , $\delta$ (FeNO)
	$\nu_{22}$		...	104	76	$\alpha$ (CFeC)
	$\nu_{23}$		...	...	149	$\beta$ (CFeN)
	$\nu_{24}$		...	100	111	$\beta'$ (CFeC)

<sup>a</sup> Mode numbering deviates from accepted convention in order to agree with that given in ref 2. <sup>b</sup>  $\nu$  denotes a stretch;  $\lambda$ ,  $\theta$ ,  $\gamma$ ,  $\alpha$ ,  $\gamma'$ ,  $\delta'$ ,  $\alpha$ ,  $\beta$ , and  $\beta'$  denote bends (Figure 3 of ref 2). <sup>c</sup> Weak and sharp peaks appear as shoulders of the stronger bands due to L( $\text{H}_2\text{O}$ ) modes on cooling. <sup>d</sup> The assignment of this band observed in ref 2 as due to  $\nu_{20}$  must be considered as incorrect in view of the polarized infrared data.

The normal-coordinate analysis, discussed in the next section, gives support to the above assignments.

**Water Bands.**—The bands due to  $\nu_1'$  and  $\nu_3'$  modes of  $\text{H}_2\text{O}$  in the spectra of the mull samples of  $\text{Na}_2\text{Fe}(\text{CN})_5\text{NO} \cdot 2\text{H}_2\text{O}$  (Table II of ref 2) are fairly broad (half-width  $\sim 20$   $\text{cm}^{-1}$ ) and give no indication of any fine structure due to correlation splitting. The  $\nu_2'$  mode, however, shows three components which were tentatively assigned to the correlation field components. The polarized infrared spectra confirm these assignments. The bands at  $\sim 3630$  and  $\sim 3550$   $\text{cm}^{-1}$  appear in all polarizations whereas the bands at  $\sim 1624$ , 1618, and 1614  $\text{cm}^{-1}$  are polarized parallel to  $c$ ,  $a$ , and  $b$  axes, respectively.

Each of the three modes of HDO appear as a doublet in the infrared spectrum of the partially deuterated sample (Table II of ref 2). The magnitude of the doublet separation is quite large amounting to 44, 31, and 13  $\text{cm}^{-1}$ , respectively, for the OH and OD stretching and the HOD bending modes. This doublet structure cannot be explained in terms of the correlation coupling because the HDO molecules exist as dilute species in the host crystal. The origin of this splitting can be ascribed to an orientation effect. Because of the low ( $C_1$ ) symmetry there are two inequivalent ways to orient the HDO molecules at the site represented by  $a$  and  $b$  below. The anisotropy of

(4) A. Sabatini, *Inorg. Chem.*, **6**, 1756 (1967).

(5) L. Tosi, *Compt. Rend.*, **264B**, 1313 (1967).

(6) R. Berreman, *Phys. Rev.*, **130**, 2193 (1963).

(7) D. Fox and R. M. Hexter, *J. Chem. Phys.*, **41**, 1125 (1964).

(8) L. Tosi, *Compt. Rend.*, **265B**, 1020 (1967).

the static field at the  $C_1$  sites results in a separation of the vibrational energy levels of the HDO molecules at



positions a and b. This effect has been termed "orientational splitting."<sup>9,10</sup> Since the a and b occupation should occur with equal probability, we can expect equal intensities of the components of each doublet. An examination of the original spectra confirmed our expectations.

**B. Vibrational Analysis.**—The results of the polarized infrared (Table I) and Raman measurements<sup>2</sup> on single-crystal sodium nitroprusside show that the static and dynamic field effects on the free ion vibrations are small since no site or correlation field splitting was observed for most of the modes, and the largest splitting was observed to be  $8\text{ cm}^{-1}$  (for  $\nu_7(A_1)$ ). Thus, it is not an unreasonable approximation to analyze the vibrational modes of  $\text{Fe}(\text{CN})_5\text{NO}^{2-}$  in the crystal lattice on the basis of "free ion"  $C_{4v}$  symmetry. Our objective was to obtain a set of calculated frequencies agreeing as closely as possible with the measured values and yielding a set of normal coordinates which agree with those assignments that have been firmly established from experimental data. The additional calculated frequencies and normal coordinates should then provide a basis for assigning the remaining bands observed in the vibrational spectra for which a certain assignment based on experimental results was not possible.

The calculations were performed using the computer programs due to Schachtschneider.<sup>11</sup> The bond distances used in computing the  $\mathbf{G}$  matrix were taken from the X-ray diffraction results given in ref 3. Mass units were taken from the 1961 international values.<sup>12</sup> The  $\mathbf{G}$  matrix was calculated for the symmetrically complete set of coordinates described previously in ref 2. This set includes three redundancies involving the  $\alpha$ ,  $\beta$ , and  $\beta'$  bends (Figure 3 of ref 2) which have the following irreducible representation under  $C_{4v}$  symmetry

$$\Gamma^{\text{red}} = 2A_1 + B_1$$

A simple modified valence force field (MVFF) was constructed using 13 valence and 7 interaction force constants (Table III). Previous calculations on the  $\text{Fe}(\text{CN})_6^{3-}$  complex by Nakagawa and Shimanouchi<sup>13</sup> provided us with some values for an initial set of force constants. This initial set was least squares refined to give the best agreement between the observed and calculated frequencies (Table II). The assignments of the calculated frequencies given in Table II were based on the potential energy distribution, except for strongly mixed modes, in which case the internal coordinate having the largest component in the corresponding

TABLE III  
FORCE CONSTANTS CALCULATED FROM THE VIBRATIONAL  
FREQUENCIES OF THE  $\text{Fe}(\text{CN})_5\text{NO}^{2-}$  ION

	Coordinate or interaction <sup>a</sup>	Value of force constant <sup>b,c</sup>
Stretch	FeN	5.407
	FeC(axial)	2.836
	NO	14.153
	CN(axial)	17.115
	FeC(radial)	1.992
Bend	CN(radial)	16.998
	$\lambda, \delta(\text{FeNO})$	0.948
	$\gamma, \delta(\text{FeCN})$	0.573
	$\lambda(\text{FeCN})$	0.297
	$\theta(\text{FeCN})$	0.470
	$\alpha(\text{CFeC})$	0.296
	$\beta'(\text{CFeC})$	0.455
	$\beta(\text{CFeN})$	0.848
	Interaction	FeC, FeC (adjacent radial)
FeC, FeC (opposite radial)		0.748
$\theta(\text{FeCN}), \theta(\text{FeCN})$ (adjacent)		-0.008
FeC(radial), $\beta'(\text{CFeC})$		0.166
FeN, FeC(axial)		0.621
FeN, NO		-0.641
	FeC(axial), $\theta(\text{FeCN})$	0.102

<sup>a</sup> Axial refers to atoms along the CNFeNO ( $C_4$ ) axis. Adjacent interaction refers to bonds joined to a common atom and inclined by  $90^\circ$ . Opposite refers to bonds joined to a common atom and inclined by  $180^\circ$ . <sup>b</sup> Stretch and stretch-stretch interaction constants in units of  $\text{mdyn}/\text{\AA}$ , bend constants in units of  $\text{mdyn } \text{\AA}/\text{radian}^2$ , and bend-stretch interaction constants in units of  $\text{mdyn}/\text{radian}$ . <sup>c</sup> The number of significant figures used in reporting the force constants is not justified by the accuracy of our experimental data. These numbers were used to calculate the frequencies given in Table II.

eigenvector was cited as the primary contributor. The calculated assignments and frequencies (Table II) are in good agreement with the assignments and observed frequencies for  $\text{Fe}(\text{CN})_5\text{NO}^{2-}$  given in Table I and in Table V of ref 2. The calculated value for the  $\nu_7(A_1)$   $\theta(\text{FeCN})$  bending mode is about 8% below the observed frequency at  $501\text{ cm}^{-1}$  (Table II) and indicates that an additional interaction constant may be important in the MVFF described in Table III. The  $\alpha$ ,  $\beta$ , and  $\beta'$  bending modes are probably strongly coupled with the external lattice modes. Consequently, the assignments of the observed low-frequency vibrations to such internal modes and a comparison with the calculated values may be without any physical significance.

The valence force constants given in Table III show some trends which we might expect based on the structure of the  $\text{Fe}(\text{CN})_5\text{NO}^{2-}$  ion in the crystal lattice.<sup>3</sup> The X-ray data show that the FeN distance ( $1.63\text{ \AA}$ ) is shorter than the FeC axial distance ( $1.90\text{ \AA}$ ), and, hence, we should expect that the FeN stretching force constant will be larger than the axial FeC stretching force constant. Because  $\beta(\text{NFeC})$  (Figure 3 of ref 2) is  $96^\circ$  in the crystal,<sup>3</sup> we should expect to find larger values for the  $\theta(\text{FeCN})$  and  $\beta'(\text{CFeN})$  bending constants compared to the  $\alpha(\text{FeCN})$  and  $\lambda(\text{CFeC})$  bending constants (Table III). This perhaps results from a comparatively higher electron density in the Fe—N=O bonds causing an appreciable nonbonded repulsive interaction with the Fe—C≡N bonds. An additional

(9) R. Kopelman, *J. Chem. Phys.*, **47**, 2631 (1967).

(10) E. R. Bernstein, *ibid.*, **50**, 4842 (1969).

(11) J. H. Schachtschneider, Technical Reports No. 231-64 and 57-65, Shell Development Co., Emeryville, Calif., 1964.

(12) "Handbook of Chemistry and Physics," 44th ed, The Chemical Rubber Publishing Co., Cleveland, Ohio, 1963, 401.

(13) I. Nakagawa and T. Shimanouchi, *Spectrochim. Acta*, **18**, 101 (1962).

effect resulting from the higher electron density in the Fe—N=O bonds would be found in a higher  $\lambda, \delta(\text{FeNO})$  bending constant as compared to, say, the  $\lambda(\text{FeCN})$  bending constant.

The interaction force constants used in the present calculation and given in Table III are those which we initially judged to be important on the basis of the  $\text{Fe}(\text{CN})_5\text{NO}^{2-}$  structure. As shown in Table III, the stretch—stretch interaction constants involving linearly related bonds are important. Initial values for stretch—stretch interactions of C—Fe—C (axial and radial), N—Fe—C, and O—N—Fe bonds (Figure 3 of ref 2) were determined from linear triatomic calculations. The

interaction constants for internal coordinates located  $90^\circ$  (adjacent) to one another are of negligible importance and can be omitted from the force field in the present calculations. As indicated in the potential energy distribution, there is some interaction between the  $\text{FeC}(\text{axial})$  and  $\theta(\text{FeCN})$  coordinates which is reflected in the small interaction constant given in Table III.

**Acknowledgment.**—The authors wish to express their gratitude to Dr. Llewellyn H. Jones for his helpful suggestions in the preparation of the manuscript for this article.

CONTRIBUTION FROM THE DEPARTMENT OF CHEMISTRY,  
IOWA STATE UNIVERSITY, AMES, IOWA 50010

## Rate and Equilibrium Studies of the Monoazidovanadium(III) Ion<sup>1a,b</sup>

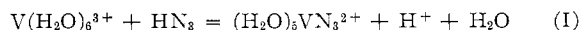
By JAMES H. ESPENSON<sup>1c</sup> AND JOHN R. PLADZIEWICZ

Received December 5, 1965

Spectral studies have verified that only a single complex with the formula  $\text{VN}_3^{2+}$  is important in  $\text{V}(\text{III})\text{--HN}_3$  solutions. Even with favorable conditions ( $1\text{ M HN}_3$ ,  $0.025\text{ M H}^+$ ) conversion of  $\text{V}^{3+}$  to  $\text{VN}_3^{2+}$  is incomplete, and no higher complexes are formed. The equilibrium quotient for the reaction  $\text{V}^{3+} + \text{HN}_3 = \text{VN}_3^{2+} + \text{H}^+$  was evaluated spectrophotometrically, and from the kinetic data,  $Q$  is  $0.016 \pm 0.002$  at  $25.0^\circ$  and  $1.00\text{ M}$  ionic strength. The rate expression is  $d[\text{VN}_3^{2+}]/dt = \{c + d/[\text{H}^+]\}[\text{V}^{3+}][\text{HN}_3] - \{a + b[\text{H}^+]\}[\text{VN}_3^{2+}]$ . Respective values of the rate parameters  $a$ ,  $b$ ,  $c$ , and  $d$  (units:  $\text{M}$  and  $\text{sec}$ ) are 3.9, 24.8, 0.39, and 0.061 at  $25.0^\circ$ . The values of  $a$  and  $b$  were also determined at other temperatures giving  $\Delta H_a^\ddagger = 15.4 \pm 0.4$  and  $\Delta H_b^\ddagger = 10.2 \pm 0.4\text{ kcal mol}^{-1}$  and  $\Delta S_a^\ddagger = -4.3 \pm 1.4$ ,  $\Delta S_b^\ddagger = -17.9 \pm 1.4\text{ cal mol}^{-1}\text{ deg}^{-1}$ . The mechanism of the reaction, particularly the question of the role of the protons in the transition states, is discussed.

### Introduction

The principal equilibrium in dilute perchloric acid solutions of vanadium(III) and hydrozoic acid involves formation of a 1:1 complex of  $\text{V}^{3+}$  and  $\text{N}_3^-$ , as represented by the net equation shown in reaction I. This



process has not been studied previously. Yet the study of the equilibrium and kinetics of this reaction is important from at least three points of view.

First, the substitution mechanism followed in  $\text{V}(\text{III})$  reactions is open to question: do these reactions follow the pattern observed for many other octahedral complexes, where bond breaking controls the energetics of the activated complex,<sup>2-6</sup> or are the features of bond

making the ones that are more important? The latter mechanism has been invoked to account for the kinetic data obtained<sup>7</sup> in a study of the reaction of  $\text{V}^{3+}$  and  $\text{NCS}^-$ . Since the reactions of  $\text{V}^{3+}$  with  $\text{NCS}^-$  and  $\text{HC}_2\text{O}_4^-$  are the only  $\text{V}(\text{III})$ -substitution processes for which data are available, it is clear that additional studies are needed to provide a clearer picture of the mechanism.

Second, the complex in question,  $\text{VN}_3^{2+}$ , is the species formed when  $\text{V}(\text{H}_2\text{O})_6^{2+}$  is oxidized, using an inner-sphere mechanism, by an azido complex.<sup>8,9</sup> Whether an inner-sphere reaction does occur is of importance in understanding  $\text{V}(\text{II})$  redox mechanisms, and for the purposes of exploring these mechanisms the kinetic and equilibrium properties of  $\text{VN}_3^{2+}$  are needed.

Third, azide ion and hydrazoic acid substitutions have been an issue of continuing interest,<sup>5,10-13</sup> particularly with regard to understanding what role the protons play in such processes.

In this paper we report results on the following as-

(1) (a) Work was performed under the auspices of the Ames Laboratory of the U. S. Atomic Energy Commission. Contribution No. 2653. (b) Presented in part at the 157th National Meeting of the American Chemical Society, Minneapolis, Minn., April 1969; see Abstracts, No. INOR 172. (c) Fellow of the Alfred P. Sloan Foundation, 1968-1970.

(2) F. Basolo and R. G. Pearson, "Mechanisms of Inorganic Reactions," 2nd ed, John Wiley and Sons, Inc., New York, N. Y., 1963.

(3) C. H. Langford and H. B. Gray, "Ligand Substitution Processes," W. A. Benjamin, Inc., New York, N. Y., 1965.

(4) J. H. Espenson, *Inorg. Chem.*, **8**, 1554 (1969), and references therein. This paper points out that although bond breaking plays an important role in  $\text{Cr}(\text{III})$  substitution, bond making is not as unimportant as it appears to be for  $\text{Fe}(\text{III})$  and  $\text{Co}(\text{III})$  substitutions.

(5) T. W. Swaddle and G. Guastalla, *ibid.*, **8**, 1604 (1969).

(6) N. Sutin, *Ann. Rev. Phys. Chem.*, **17**, 119 (1966).

(7) B. R. Baker, N. Sutin, and T. J. Welch, *Inorg. Chem.*, **6**, 1948 (1967).

(8) J. H. Espenson, *J. Am. Chem. Soc.*, **89**, 1276 (1967).

(9) K. M. Davies and J. H. Espenson, *ibid.*, **91**, 3093 (1969).

(10) D. W. Carlyle and J. H. Espenson, *Inorg. Chem.*, **6**, 1370 (1967).

(11) D. Seewald and N. Sutin, *ibid.*, **2**, 643 (1963).

(12) T. W. Swaddle and E. L. King, *ibid.*, **3**, 234 (1964).

(13) F. Accascina, F. P. Cavasino, and S. D'Alessandro, *J. Phys. Chem.*, **71**, 2474 (1967).